Hindawi
Stem Cells International
Volume 2024, Article ID 9820256, 1 page
https://doi.org/10.1155/2024/9820256

Retraction

Retracted: Human Umbilical Mesenchymal Stem Cells-Derived Microvesicles Attenuate Formation of Hypertrophic Scar through Multiple Mechanisms

Stem Cells International

Received 30 January 2024; Accepted 30 January 2024; Published 31 January 2024

This article has been retracted by Hindawi following an investigation undertaken by the publisher [1]. This investigation has uncovered evidence of one or more of the following indicators of systematic manipulation of the publication process:

(1) Discrepancies in scope
(2) Discrepancies in the description of the research reported
(3) Discrepancies between the availability of data and the research described
(4) Inappropriate citations
(5) Incoherent, meaningless and/or irrelevant content included in the article
(6) Manipulated or compromised peer review

The presence of these indicators undermines our confidence in the integrity of the article's content and we cannot, therefore, vouch for its reliability. Please note that this notice is intended solely to alert readers that the content of this article is unreliable. We have not investigated whether authors were aware of or involved in the systematic manipulation of the publication process.

Wiley and Hindawi regrets that the usual quality checks did not identify these issues before publication and have since put additional measures in place to safeguard research integrity.

We wish to credit our own Research Integrity and Research Publishing teams and anonymous and named external researchers and research integrity experts for contributing to this investigation.

The corresponding author, as the representative of all authors, has been given the opportunity to register their agreement or disagreement to this retraction. We have kept a record of any response received.

References

[1] Q. Qian, N. Zhu, W. Li et al., "Human Umbilical Mesenchymal Stem Cells-Derived Microvesicles Attenuate Formation of Hypertrophic Scar through Multiple Mechanisms," *Stem Cells International*, vol. 2023, Article ID 9125265, 15 pages, 2023.

Hindawi
Stem Cells International
Volume 2023, Article ID 9125265, 15 pages
https://doi.org/10.1155/2023/9125265

Research Article

Human Umbilical Mesenchymal Stem Cells-Derived Microvesicles Attenuate Formation of Hypertrophic Scar through Multiple Mechanisms

Qun Qian,[1] Ni Zhu,[2,3] Wenzhe Li,[1] Songlin Wan,[1] Dongcheng Wu,[4] Yunhua Wu,[1] and Weicheng Liu[1]

[1]*Zhongnan Hospital of Wuhan University, Clinical Center for Pelvic Floor Surgery, Department of Colorectal and Anal Surgery, Clinical Center of Intestinal and Colorectal Diseases of Hubei Province, Key Laboratory of Intestinal and Colorectal Diseases of Hubei Province, Wuhan University, Wuhan, Hubei, China*
[2]*Institute of Medical Virology, School of Basic Medical Sciences, Wuhan University, Wuhan, Hubei, China*
[3]*Research Center of Basic Medical Sciences, School of Basic Medical Sciences, Xianning Medical College, Hubei University of Science and Technology, Xianning, Hubei, China*
[4]*Department of Biochemistry and Molecular Biology, School of Basic Medical Sciences, Wuhan University, Wuhan, Hubei, China*

Correspondence should be addressed to Weicheng Liu; wb000837@whu.edu.cn

Received 6 September 2022; Revised 20 October 2022; Accepted 31 March 2023; Published 15 July 2023

Academic Editor: A. S. M. Golam Kibria

Mesenchymal stem cells and the derived extracellular microvesicles are potential promising therapy for many disease conditions, including wound healing. Since current therapeutic approaches do not satisfactorily attenuate or ameliorate formation of hypertrophic scars, it is necessary to develop novel drugs to achieve better outcomes. In this study, we investigated the effects and the underlying mechanisms of human umbilical mesenchymal stem cells (HUMSCs)-derived microvesicles (HUMSCs-MVs) on hypertrophic scar formation using a rabbit ear model and a human foreskin fibroblasts (HFF) culture model. The results showed that HUMSCs-MVs reduced formation of hypertrophic scar tissues in the rabbit model based on appearance observation, and hematoxylin and eosin (H&E), Masson, and immunohistochemical stainings. HUMSCs-MVs inhibited invasion of HFF cells and decreased the levels of the α-SMA, N-WASP, and cortacin proteins. HUMSCs-MVs also inhibited cell proliferation of HFF cells. The MMP-1, MMP-3, and TIMP-3 mRNA levels were significantly increased, and the TIMP-4 mRNA level and the NF-kB p65/β-catenin protein levels were significantly decreased in HFF cells after HUMSCs-MVs treatment. The p-SMAD2/3 levels and the ratios of p-SMAD2/3/SMAD2/3 were significantly decreased in both the wound healing tissues and HFF cells after HUMSCs-MVs treatment. CD34 levels were significantly decreased in both wound healing scar tissues and HFF cells after HUMSCs-MVs treatment. The VEGF-A level was also significantly decreased in HFF cells after HUMSCs-MVs treatment. The magnitudes of changes in these markers by HUMSCs-MVs were mostly higher than those by dexamethasone. These results suggested that HUMSCs-MVs attenuated formation of hypertrophic scar during wound healing through inhibiting proliferation and invasion of fibrotic cells, inflammation and oxidative stress, Smad2/3 activation, and angiogenesis. HUMSCs-MVs is a potential promising drug to attenuate formation of hypertrophic scar during wound healing.

1. Introduction

Mesenchymal stem cells (MSCs) are multipotent cells and play important roles in tissue generation, immunomodulation, and inflammation and oxidative stress resolves. Although there are concerns about safety and complex mechanisms of long-term use, the MSCs have shown promising potentials in therapy of many diseases, including cardiac neurological, and orthopedic disorders [1–4].

Hypertrophic scars formation after injury, burn, and surgery is a disease characterized by disorder in excess extracellular matrix (ECM) deposition and remodeling, abnormal angiogenesis, inflammation, overly activated fibroblasts and excessive fibrosis, and migration of abnormal types and numbers of cells

into the wound. These processes involve genetic, local mechanical, and systemic factors such as circulating cytokines, chemokines, and growth factors during formation of hypertrophic scars [5–7]. Several therapeutic approaches including surgical excision, laser therapy, avotermin, heparin gel application, silicon-containing dressings, intralesional corticosteroid, and pressure therapy have been applied to treat hypertrophic scars. However, they do not satisfactorily attenuate or ameliorate formation of hypertrophic scars for several reasons, such as low efficacy, side effects, high cost, and nonetiological treatment [8–11]. MSCs including bone marrow-derived mesenchymal stem cells, adipose tissue-derived mesenchymal stem cells (ADSCs), and human umbilical mesenchymal stem cells (HUMSCs) are proven to attenuate formation of hypertrophic scars without complications in terms of macroscopic and histological appearances through several mechanisms, such as regulating inflammation [12–18]. Signaling pathways such as p38/MAPK pathway [19] and TGF beta1/Smad3 pathway [20] are also involved in regulating their efficacy on treatment of hypertrophic scars. MSCs or MSC-conditioned media have emerged as a promising cell-based therapy for alleviating hypertrophic scars.

Extracellular vesicles are derived from cells. They contained paracrine factors of cells and have been found to be functional in treating many disorders. Extracellular vesicles are considered as a safer approach than MSCs because they lack activity of living cells such as proliferation and migration. A recent study showed that extracellular vesicles derived from human ADSCs prevent the formation of hypertrophic scars in a rabbit model [21]. Compared with other MSCs used in therapy, HUMSCs has several advantages, including high differentiative potential, less immune-rejection, availability with less legal or ethical issues, rich sources for collection [22–25]. The effects and underlying mechanisms of HUMSCs-derived extracellular vesicles on hypertrophic scars remain unclear.

In this study, we investigated the effects and the underlying mechanism of HUMSCs-MVs on formation of hypertrophic scars using a rabbit ear model and a human foreskin fibroblast (HFF) model. The rabbit ear model has been applied in drug discovery for hypertrophic scar in many studies for its reproducibility to the pathophysiology of hypertrophic scar formation in human with low cost [21, 26–28]. As the most common cells of the connective tissue, fibroblasts are heterogeneous and can proliferate and migrate to the injury site. They play a key role in wound healing by secreting or breaking down collagen, glycoproteins, glycosaminoglycans, and fibers of the ECM [29, 30]. HFF is a type of fibroblasts derived from foreskin tissues discarded after surgery. They have been used or proposed to use in several areas of research and medicine, including uses in cellular damage and mitochondrial dysfunction tests of toxins, feeder cells for stem cells, and wound healing [31–34]. Our data indicated that HUMSCs-MVs effectively reduced formation of hypertrophic scar tissues probably through inhibiting proliferation and invasion of fibroblasts, resolving inflammation and oxidative stress, suppressing Smad2/3 activation, and reducing angiogenesis. Therefore, HUMSCs-MVs is a potential promising drug to attenuate formation of hypertrophic scar during wound healing.

2. Materials and Methods

2.1. Preparation of HUMSCs-MVs. HUMSCs were obtained from Cyagen Biosciences Inc. (Cat. No. HUXUC-01001, Sunnyvale, CA, USA) and cultured in α-MEM medium (Cyagen Biosciences Inc.). Medium was replaced using FBS-free α-MEM when HUMSCs reached 70%–80% confluency. The medium was collected after 48 hr. MVs were prepared from the collected medium by following the published protocols [35, 36]. The precipitate was resuspended using 13 ml PBS. Finally, the precipitate was resuspended using 100 μl PBS. The contains of total proteins in MVs were determined using the Bradford assay using the BCA kit (Takara, Japan) as the concentration of the HUMSCs-MVs. The recovery of HUMSCs-MVs from HUMSCs was 875.43 μg/50 ml media for 4×10^7 cells in five 10-cm dishes. To observe MVs, the prepared MVs were dissolved in PBS, loaded onto copper grids, stained using 1% (w/v) phosphotungstic acid, and then examined using a transmission electron microscope (Model; TECNAI-10, Philips, Holland). CD44 and CD29 in MVs were determined using Western blotting.

2.2. Animal Model Study. A total of eight male rabbits (varieties: New Zealand White rabbits) weighed 2,000–3,000 g were purchased from Chongqing Ensiweier Biotech. Co. Ltd., Chongqing, China. The hypertrophic scar model was constructed by following the published studies [37, 38]. In brief, the rabbits were anesthetized using 1% pentobarbital sodium at dosage of 40 mg/kg. Four circular surgical areas each with a diameter of 1 cm were designed with a drilling instrument on each ear the ventral surface of rabbit. The skin in the surgical area was cut to the cartilage with a scalpel, then cut along the designed circular position with ophthalmic scissors and ophthalmic forceps to expose the cartilage layer. The cartilage membrane was removed with ophthalmic forceps and ophthalmic scissors. On postoperative day 1, day 7, day 14, and day 28, following formation of rabbit hypertrophic scars, scars in eight rabbits (with 32 left and 32 right, total of 64 scars) were divided into four groups, including (1) the PBS group (16 scars), where scars were treated only with PBS, (2) the MVs group (16 scars), where scars were treated with 100 μl HUMSCs-derived MVs (containing about 100 μg MVs) at day 1, day 7, day 14, and day 28, (3) the ointment group (16 scars), where scars were treated with the ointment that was made according to a prescription of Traditional Chinese Medicine every day, and (4) the dexamethasone (DEX) group (16 scars), where scars were treated with DEX at dosage of 1 mg/1,000 g at day 1, day 7, day 14, and day 28. Tissues samples in all four groups were harvested on day 30. The animal model study was approved by corresponding author's institution and conducted by following guidelines for laboratory animal care and use. We do not elaborate the data on the Ointment group in this study for the related results are incomplete.

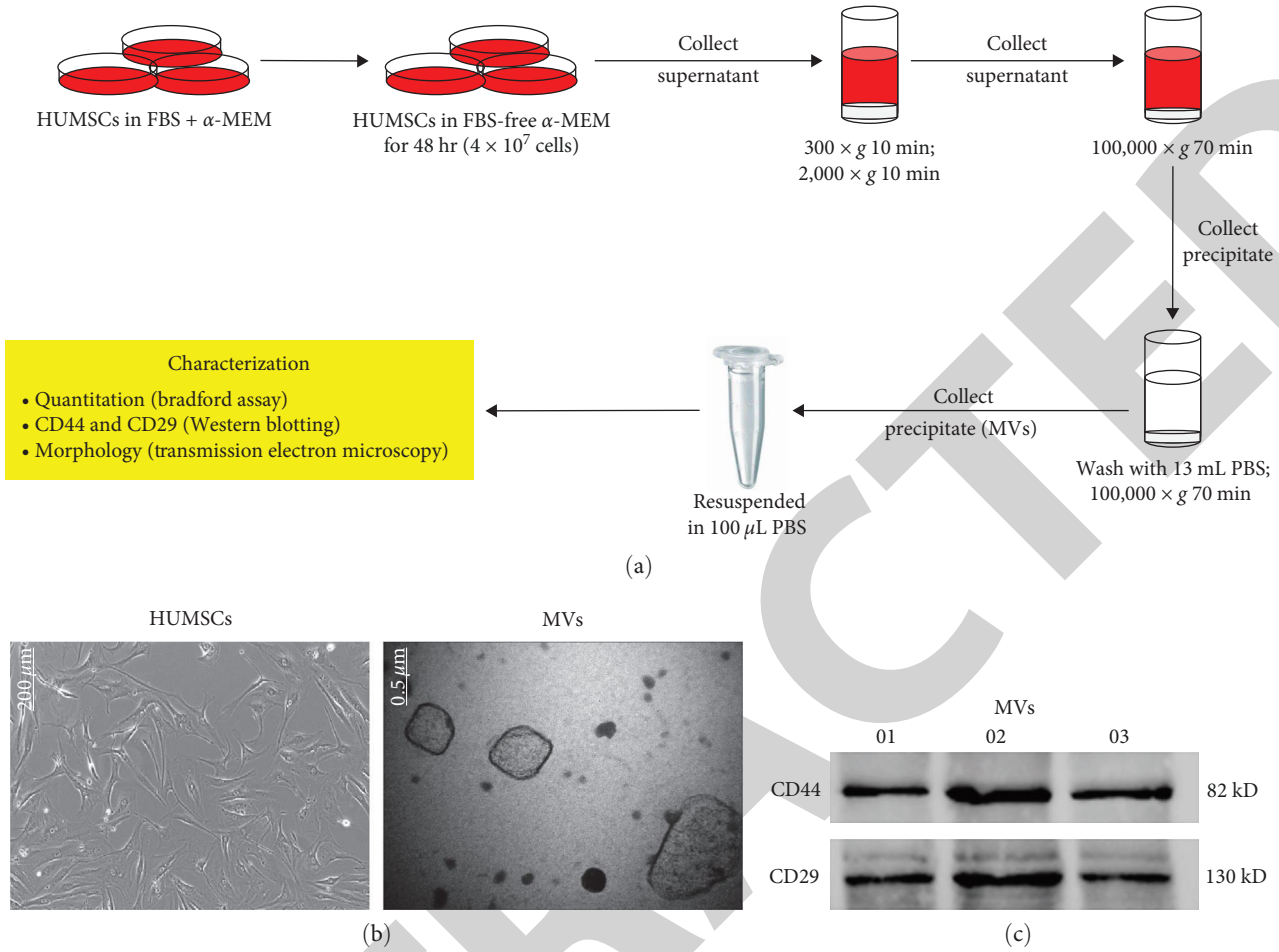

Figure 1: Preparation and characterization of the HUMSCs-derived MVs (HUMSCs-MVs). (a) Preparation of MVs from HUMSCs. The HUMSCs-MVs was prepared from media of HUMSCs culture. (b) Visualization of HUMSCs-MVs using an electronic microscope. (c) HUMSCs-MVs contained CD44 and CD29. CD44 and CD29 in HUMSCs-MVs were determined using Western blotting assay.

2.3. Histological Examination. Tissue sections in 5 μm thick were obtained and used for H&E staining, Masson staining, and immunohistochemical staining. Hematoxylin (Jiancheng Biotech. Co. Ltd., Nanjing, China) and eosin were applied for 10 min and 30 s, respectively, in H&E staining. The Masson Staining Kit (Cat. No. DC0032, Leagene Biotech. Co. Ltd.,) was used for Masson staining. For the immunohistochemical staining, the sections were treated with 3% hydrogen peroxide. Afterward, the sections were incubated with rabbit anti-α-SMA antibody (1 : 1,000, Abcam Biotech., Cambridge, MA, USA) at 4°C overnight. The stained sections were observed and recorded using a microscope (CK-40, OLYMPUS, Japan).

2.4. Cell Culture and Treatment. According to the needs of research, the HFF cells were divided into three groups: (1) the PBS group, where HFF cells were treated with PBS, (2) the MVs group, where HFF cells were treated with 30, 60, and/or 90 μg/ml MVs, (3) the DEX group, where HFF cells were treated with 30 μg/ml dexamethasone (DEX).

2.5. Proliferation Assay of Human Foreskin Fibroblast (HFF). The proliferation of HFF cells was determined using a CCK-8 kit (Beyotime Biotech). The HFF cells were seeded in a 96-well plate at a density of 1×10^5/ml and incubated for 24 hr at 37°C. An aliquot of 10 μl CCK-8 solution was then added to the HFF cells and incubated for 3 hr at 37°C. After shaking for 10 min, the absorbance at the wavelength of 450 nm (representing cell viability) was measured using a spectrophotometer.

2.6. Invasion Assay. The transwell invasion assay using Transwell (pore size 8 μm, Costar, USA) was performed to examine the invasion potential of HFF cells. HFF cells (5×10^4 cells in 200 μl serum-free medium) were added to the upper chamber and 600 μl medium containing 10% FBS and 90 μg/ml MVs or 30 μg/ml DEX was added to the lower chamber. After 24 hr, the invaded HFF cells on membrane were fixed using 4% paraformaldehyde (Sinopharm. Group, Shanghai, China) for 20 min, followed by staining with 1% crystal violet staining solution (Shanghai Gefen Biotech. Co. Ltd., Shanghai, China) for 15 min. Finally, the stained HFF cells were visualized and recorded using a fluorescence microscope (CK-40, OLYMPUS, Nikon, Japan).

2.7. ELISA Assay. ELISA assay was used to determine malondialdehyde (MDA) levels, superoxide dismutase (SOD) activity, and VEGF-A levels in hypertrophic scar tissues or HFF cells. The supernatants were collected after

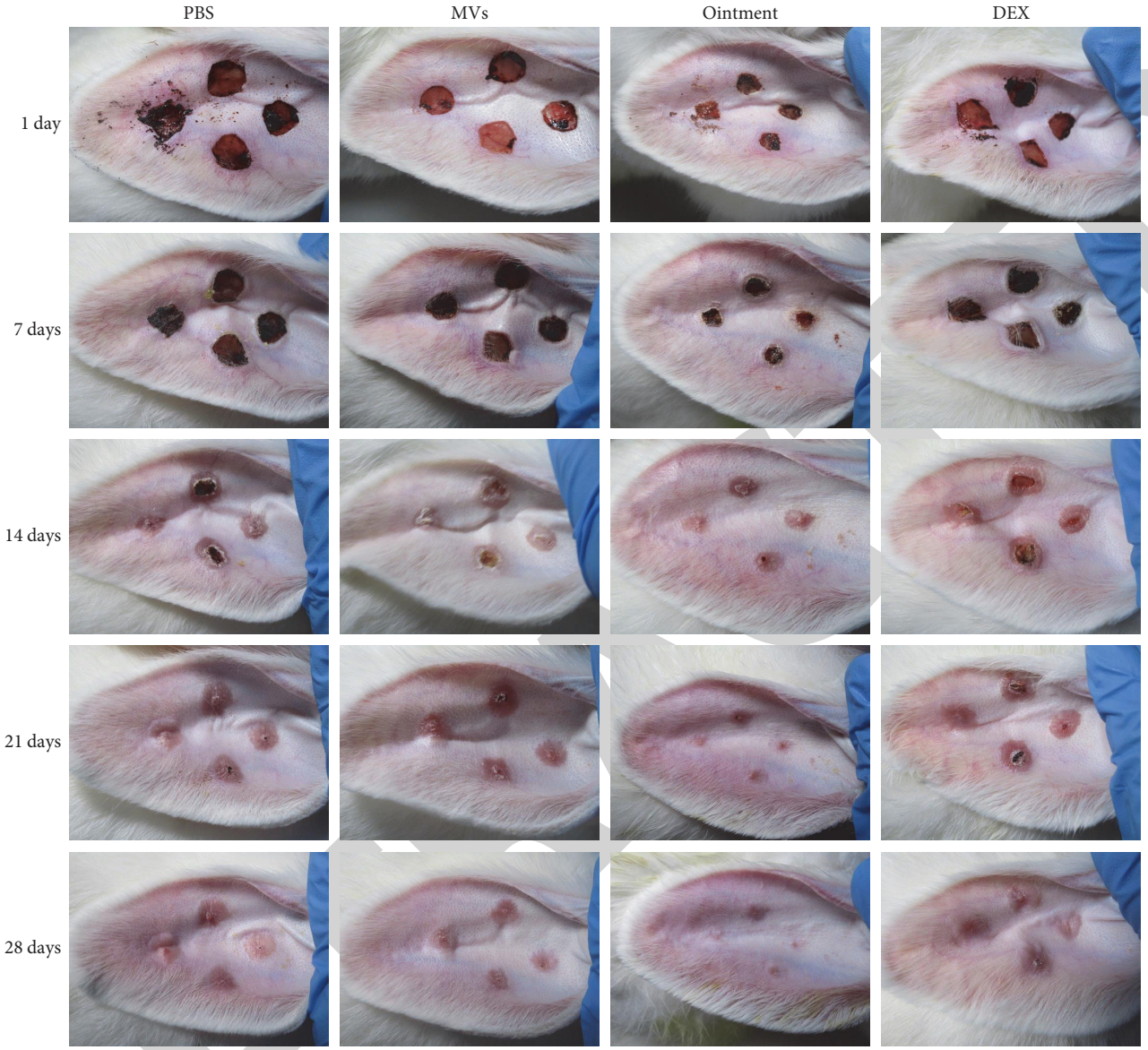

Figure 2: HUMSCs-MVs attenuated formation of hypertrophic scar tissues in the rabbit ear model. Wounds in a rabbit model were treated with PBS, HUMSCs-MVs, ointment, and DEX tissues were examined. The recovering scars were examined and appearance was recorded with photos at 1, 7, 14, 21, and 28 days after the scar models were established.

centrifugation and subjected to determine MDA levels, SOD activity, and VEGF-A levels using an MDA assay kit (Cat. No. A003-1-2, Jiancheng Biotech. Co. Ltd.) and a SOD assay kit (Cat. No. A001-3-2, Jiancheng Biotech. Co. Ltd.), a VEGF-A assay kit (Cat# ml060752, Mlbio, China), respectively.

2.8. Quantitative Real Time-Polymerase Chain Reaction (qRT-PCR) Assay. The total RNA of the HFF cells was isolated using the TaKaRa MiniBEST Universal RNA Extraction Kit (Cat. No. 9767, Takara, Takara Bio, Japan) and the complementary DNA (cDNA) was synthesized with the PrimeScript™ II 1st Strand cDNA Synthesis Kit (Cat. No. 6210A, Takara Bio.) as instructed by protocols of the manufacturers. The RT-PCR was conducted in the AB Step One plus Real-Time PCR System. Primers were synthesized in General Bio (Anhui, China). The sequences of primers included MMP-1-F, 5′-AGCTAGCTCAG GATGACATTGATG-3′, MMP-1-R, 5′-GCCGATGGGCTG GACAG-3′, MMP-3-F, 5′-ATTCCATGGAGCCAGGCTTTC-3′, MMP-3-R, 5′-CATTTGGGTCAAACTCCAACTGTG-3′, TIMP-3-F, 5′-TCTGCAACTCCGACATCGTG-3′, TIMP-3-R, 5′-CGGATGCAGGCGTAGTGTT-3′, TIMP-4-F, 5′-CACCCT CAGCAGCACATCTG-3′, TIMP-4-R, 5′-GGCCGGAACT ACCTTCTCACT-3′. GAPDH-F, 5′-AGAAGGCTGGGGCTC ATTTG-3′, GAPDH-R, 5′-AGGGGCCATCCACAGTCTTC-3′. The GAPDH gene was used as the internal control.

2.9. Western Blotting. Hypertrophic scar tissues were homogenized using RIPA buffer (100 mg/ml). The supernatants were collected and quantified. The protein samples with 20 μg protein each were resolved in the 10% SDS–PAGE by electrophoresis

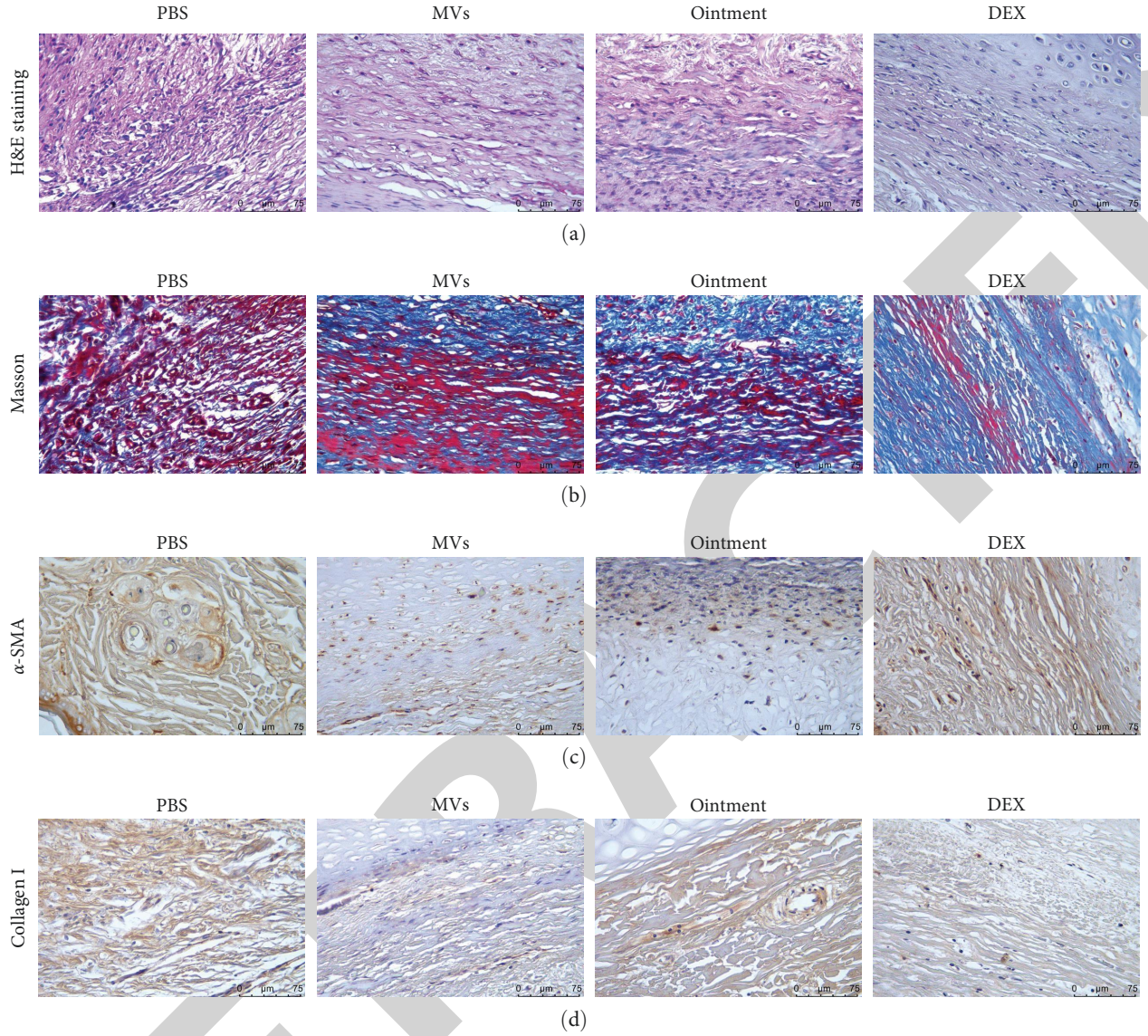

FIGURE 3: Pathological examination of hypertrophic scar tissues in the rabbit ear model treated with PBS, HUMSCs-MVs, ointment, and DEX. Hypertrophic scar tissues were sectioned and examined by pathological staining. (a) H&E staining to reveal changes in fibrotic tissues in scar tissues treated with PBS, HUMSCs-MVs, ointment, and DEX. (b) Masson staining to reveal changes in collagen fibers in scar tissues treated with PBS, HUMSCs-MVs, ointment, and DEX. (c, d) The immunohistochemical staining to reveal α-SMA (c) and collagen I (d) expression. Magnification, 400x.

and then electrotransferred to the polyvinylidene fluoride membranes. The signals were detected using the ECL solution (Applygen, Beijing, China) and recorded and analyzed using Tanon Image Analysis System (Model: Tanon 4800, Shanghai Tanon Tech. Co. Ltd., Shanghai, China). The primary antibodies used in Western blotting included rabbit anti-Nrf2 antibody (Cat#ab62352), anti-SMAD2/3 of rabbit (Cat#ab202445), anti-p-SMAD2/3 of rabbit (Cat#ab272332), anti-CD34 of rabbit (Cat#ab110643), anti-β-catenin of rabbit antibody (Cat#ab32572), anti-NF kB p65 of rabbit antibody (Cat#ab16502), rabbit anti-α-SMA antibody (dilution, Cat#ab5694), rabbit anti-N-WASP antibody (dilution, Cat#ab126626), anticortacin antibody of rabbit (Cat#ab81208), and rabbit anti-GAPDH (0 dilution, Cat#ab22555).

2.10. Statistical Analysis. Data were represented as mean ± standard deviation and analyzed with SPSS 16.0. One-way ANOVA was applied to evaluate the statistical significance of differences among groups.

3. Results

3.1. Characterization of the HUMSCs-MVs. MVs were prepared from the medium of HUMSCs cultures (Figure 1(a)). We found that the HUMSCs-MVs were round-shaped membrane vesicles with diameters in the range of 300–500 nm under the electron microscope (Figure 1(b)). The Western blotting showed that HUMSCs-MVs obviously contained CD44 and

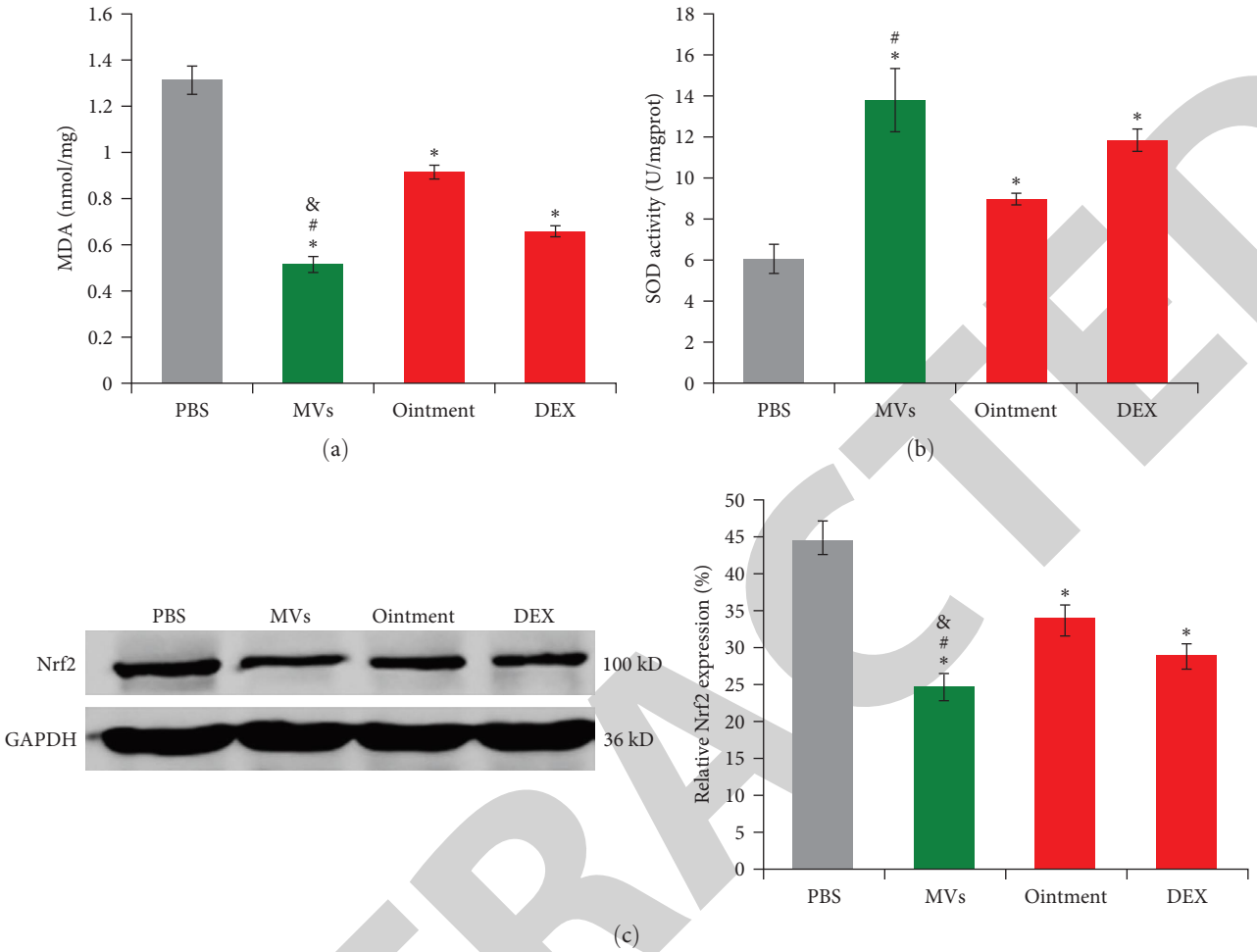

FIGURE 4: HUMSCs-MVs inhibited oxidative stress in wound healing scar tissues in the rabbit ear model. (a) HUMSCs-MVs decreased the MDA levels in scar tissues. The MDA levels were determined by ELISA. (b) HUMSCs-MVs increased the SOD activity in scar tissues. The SOD activity was determined by ELISA. (c) HUMSCs-MVs decreased the expression of Nrf2 in scar tissues. The expression of Nrf2 was determined using Western blotting. $^*P<0.05$ compared with the PBS group. $\#P<0.05$ compared with the ointment group. $\&P<0.05$ vs. compared with the DEX group.

CD29 (Figure 1(c)), confirming the identity of HUMSCs-MVs. We used these HUMSCs-MVs for subsequent studies.

3.2. HUMSCs-MVs Reduced Formation of Hypertrophic Scar Tissues in a Rabbit Model. To examine the effects of HUMSCs-MVs on formation of hypertrophic scar tissues, we generated hypertrophic scars in the ear of rabbits and treated the scars with HUMSCs-MVs, or dexamethasone (DEX), and PBS. DEX is a known drug to attenuate hypertrophic scars, which has been used in research [39–41]. The results showed that the raised and hard hypertrophic scars were present in the healing wound areas in the rabbit earlobes treated with PBS on the 7th day (Figure 2). The scar tissues in the DEX group were softer in the 14th day than those in the PBS group and similar to those treated with PBS in the other days examined (Figure 2). The scars in the MVs treatment group were softer and smaller than those in the PBS group and the DEX group (Figure 2). These results suggested that HUMSCs-MV inhibited formation of hypertrophic scar tissues and the inhibitory effects were better than that of DEX.

We further evaluated the effects of HUMSCs-MVs on the formation of hypertrophic scars using H&E staining, Masson staining, and immunohistochemical assay. H&E staining assay showed that scar tissues in the HUMSCs-MVs treated group were flatter in the dermal layer compared with those in the PBS group (Figure 3). Irregular fibroblasts, angiogenesis, and the dermis layer were found, and they were attenuated in the HUMSCs-MVs treatment group (Figure 3(a)). The Masson staining assay showed that the collagen fibers were irregularly arranged, thick and densely packed in scar tissues of the PBS group, while the collagen fibers were arranged in a more organized manner in scar tissues of the HUMSCs-MVs group (Figure 3(b)). The immunohistochemistry assay showed that the expression of α-SMA (Figure 3(c)) and collagen I (Figure 3(d)) in scar tissues of the HUMSCs-MVs group was obviously decreased compared with those in the PBS group. Interestingly, the inhibitory effects on pathological changes of formation of hypertrophic scars by HUMSCs-MVs were even better than those by DEX in the H&E staining, Masson staining, and immunohistochemical results (Figure 3(a)–3(d)). These

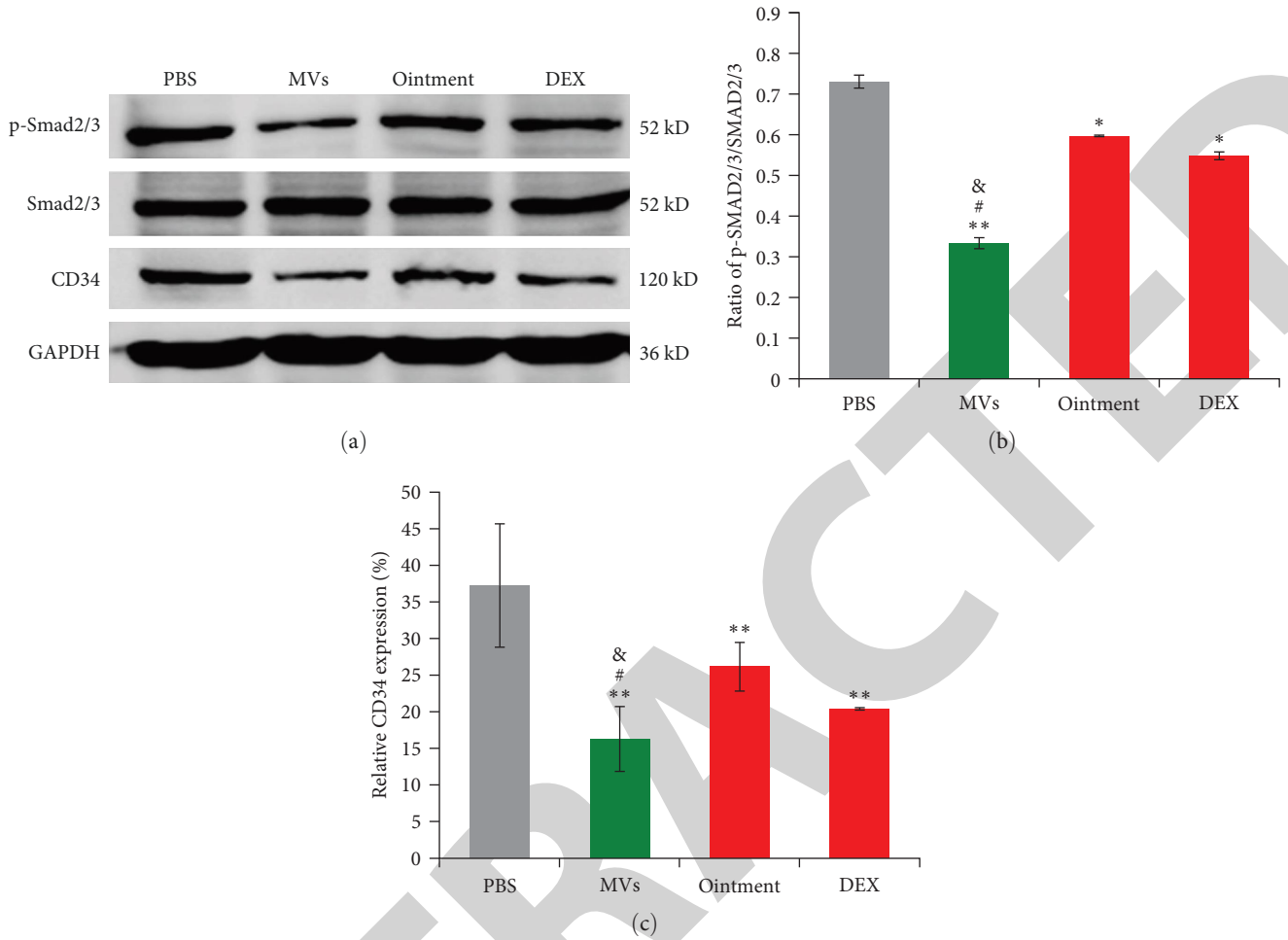

Figure 5: HUMSCs-MVs decreased phosphorylation of SMAD2/3 and the CD34 level in wound healing scar tissues in the rabbit ear model. (a) SMAD2/3, p-SMAD2/3, CD34, and GAPDH were determined using Western blotting. GAPDH was used as loading control. (b) Quantitation analysis of ratios of p-SMAD2/3/SMAD2/3 in the results of Western blotting. (c) Quantitation analysis of the CD34 protein levels in the results of Western blotting. $^{*}P<0.05$ and $^{**}P<0.01$ compared with the PBS group. $\#P<0.05$ compared with the ointment group. $\&P<0.05$ compared with the DEX group.

results suggested that HUMSCs-MVs attenuated formation of hypertrophic scar and the efficacy was better than that of DEX.

3.3. HUMSCs-MVs Inhibited Oxidative Stress in Wound Healing Scar Tissues in a Rabbit Model. Oxidative stress is associated with hypertrophic scar formation [42]. To investigate the effect of HUMSCs-MVs on oxidative stress during scar formation, we determined the levels of oxidative stress biomarkers MDA, SOD, and Nrf2 in the scar tissues of the rabbit model treated with PBS, HUMSCs-MVs, ointment, or DEX. The results showed that the MDA levels in scar tissues treated with HUMSCs-MVs or DEX were significantly decreased (Figure 4(a)). The SOD activity in scar tissues treated with HUMSCs-MVs or DEX was significantly increased (Figure 4(b)). The Nrf2 expression levels in scar tissues treated with HUMSCs-MVs or DEX were significantly decreased (Figure 4(c)). The changes in MDA levels, SOD activity, and Nrf2 expression levels in scar tissues were or tended to be even higher in the HUMSCs-MVs group than those in the DEX group (Figure 4(a)–4(c)). These results suggested that HUMSCs-MVs attenuated hypertrophic scars through inhibiting oxidative stress.

3.4. HUMSCs-MVs Suppressed SMAD2/3 Signaling in Wound Healing Scar Tissues in a Rabbit Model. Smad signaling pathway is the most canonical pathway involved in collagen production and hypertrophic scars formation [43]. To investigate the potential role of Smad signaling underlying the effect of HUMSCs-MVs in suppressing scar formation, we determined phosphorylation levels of SMAD2/3 in the scar tissues of the rabbit model treated with PBS, HUMSCs-MVs, or DEX using Western blotting, since SMAD2/3 plays critical roles in collagen production and formation of hypertrophic scars. No significant difference in the levels of SMAD2/3 among the PBS, HUMSCs-MVs, and DEX groups. The levels and ratios of p-SMAD2/3/SMAD2/3 were significantly decreased in the HUMSCs-MVs and DEX groups, compared with the PBS group (Figures 5(a) and 5(b)). The level and the ratios of p-SMAD2/3/SMAD2/3 were even significantly lower in the HUMSCs-MVs group than those in the DEX group (Figures 5(a) and 5(b)). These results suggested that HUMSCs-MVs attenuated hypertrophic scars through inhibiting phosphorylation of SMAD2/3.

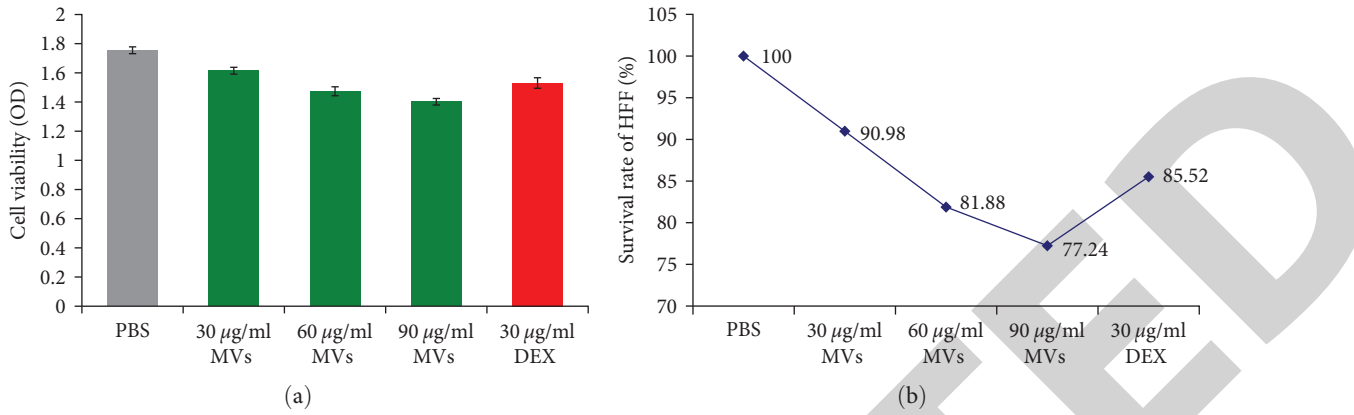

Figure 6: HUMSCs-MVs inhibited the proliferation of HFF cells. HFF cells were treated with PBS, HUMSCs-MVs, and DEX and then subjected to viability assay using a CCK-8 kit. (a) The OD values of viability analysis of HFF cells treated with PBS, HUMSCs-MVs, and DEX using CCK-8 assay. (b) The survival rates of HFF cells treated with PBS, HUMSCs-MVs, and DEX using CCK-8 assay.

3.5. HUMSCs-MVs Inhibited CD34 Expression in Wound Healing Scar Tissues in a Rabbit Model. CD34 is a biomarker and involved in initial angiogenesis [44, 45] which is a key process in early stage of formation of hypertrophic scar [5–7]. To investigate the effect of HUMSCs-MVs on angiogenesis during scar formation, we determined CD34 levels in the scar tissues of the rabbit model treated with PBS, HUMSCs-MVs, ointment, or DEX using Western blotting. The results showed that the CD34 levels were decreased in the HUMSCs-MVs, and DEX groups, compared with the PBS group (Figures 5(a) and 5(c)). The CD34 level was even lower in the HUMSCs-MVs group than that in the DEX group (Figures 5(a) and 5(c)). These results suggested that HUMSCs-MVs attenuated hypertrophic scars through inhibiting angiogenesis.

3.6. HUMSCs-MVs Inhibited Proliferation and Invasion of HFF Cells. Abnormal migration and invasion of fast proliferation of fibroblasts in wound healing tissues are characteristics of hypertrophic scars [5–7, 46]. To further investigate the potential mechanism underlying the ameliorative effects of HUMSCs-MVs on hypertrophic scars, we examined the effects of HUMSCs-MVs on proliferation and invasion of fibroblasts that are key component of hypertrophic scars using HFF as a model. The proliferation of HFF cells was examined using the CCK-8 assay. The invasion of HFF cells was examined using Transwell assays and determination of the protein levels of the invasion biomarkers α-SMA, N-WASP, and cortacin. The results showed that treatment with HUMSCs-MVs or DEX resulted in decreases in the viability of HFF cells, compared with the PBS treatment. The suppression by HUMSCs-MVs was dose-dependent (Figures 6(a) and 6(b)). HUMSCs-MVs and DEX inhibited invasion of HFF cells, compared with PBS (Figures 7(a) and 7(b)). The magnitude of change in the invasion levels was lower in the group of HUMSCs-MVs than that in the group of DEX, and the difference was not significant (Figures 7(a) and 7(b)). Consistently, HUMSCs-MVs and DEX treatment resulted in decreases in the α-SMA, N-WASP, cortacin protein levels, compared with those of PBS treatment (Figure 7(c)–7(f)). The magnitude of changes in the α-SMA, N-WASP, cortacin protein levels was lower in the HUMSCs-MVs (Figure 7(c)–7(f)). These results suggested that HUMSCs-MVs inhibited proliferation and invasion of HFF cells.

3.7. HUMSCs-MVs Inhibited SMAD2/3 Signaling and CD34 and VEGF-A Levels in HFF Cells. Smad signaling pathway is the most canonical pathway involved in collagen production and hypertrophic scars formation [43]. To further investigate the role of Smad signaling pathway underlying the ameliorative effects of HUMSCs-MVs on hypertrophic scars, we determined the phosphorylation levels of SMAD2/3 in HFF cells using Western blotting. The results showed that there was no significant difference in the levels of SMAD2/3 among the PBS, HUMSCs-MVs, and DEX groups. The p-SMAD2/3 levels were significantly decreased in the HUMSCs-MVs and DEX groups compared with that in the PBS group (Figures 8(a) and 8(b)). The p-SMAD2/3 level and the ratio of p-SMAD(2/3)/SMAD(2/3) were even significantly lower in the HUMSCs-MVs group than those in the DEX group (Figures 8(a) and 8 (b)). These results suggested that HUMSCs-MVs inhibited collagen formation through inhibiting activation of SMAD2/3.

CD34 is involved in initial angiogenesis [44, 45] and VEGF-A is a key regulator of angiogenesis [47, 48]. To further investigate the role of angiogenesis underlying the ameliorative effects of HUMSCs-MVs on hypertrophic scars, we determined CD34 and VEGF-A levels in HFF cells using Western blotting and ELISA assay. The results showed that the CD34 protein levels (Figures 8(a) and 8(c)) and the VEGF-A protein levels (Figure 8(d)) were significantly decreased in the HUMSCs-MVs and DEX groups, compared with the PBS group. The CD34 level and the VEGF-A level were or tended to be significantly lower in the HUMSCs-MVs group than those in the DEX group (Figure 8(a)–8(d)). These results suggested that HUMSCs-MVs inhibited angiogenesis from HFF cells.

3.8. HUMSCs-MVs Decreased Inflammation in HFF Cells. Chronic inflammation is a key factor contributing to formation of hypertrophic scars [6, 7]. NF-kB is a master regulator of genes involved in inflammation [49, 50]. β-catenin is the downstream component of Wnt/β-catenin pathway that crosstalks with NF-kB signaling pathway during inflammation [51]. MMPs and TIMPs are key components of tissue remodeling

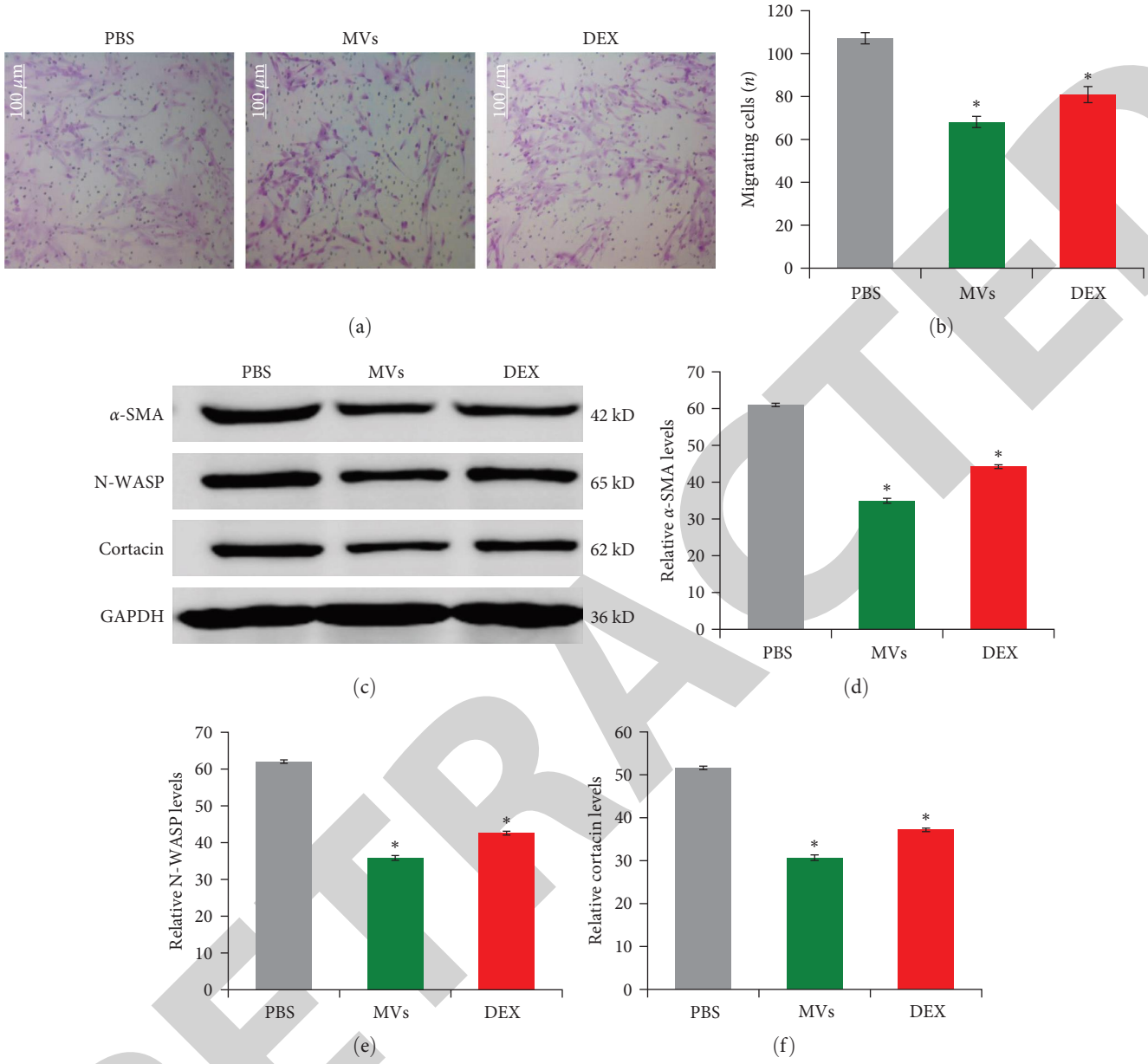

Figure 7: HUMSCs-MVs inhibited invasion of HFF cells. HFF cells were treated with PBS, HUMSCs-MVs, and DEX and subjected to analysis of invasion potentials and determination of the α-SMA, N-WASP, cortacin, GAPDH protein levels using Western blotting. (a) The representative results of invasion assay using matrigels. Magnification, 400x. (b) Quantitative analysis of invasion assay. (c) α-SMA, N-WASP, cortacin, and GAPDH protein levels were determined using Western blotting. GAPDH was used as loading control. (d–f) Quantitation analysis of the α-SMA, N-WASP, and cortacin protein levels in the results of Western blotting. $^*P<0.05$, compared with the PBS group.

in inflammation [52–54]. To investigate the role of inflammation underlying the ameliorative effects of HUMSCs-MVs on hypertrophic scars, we determined both NF-kB p65 and β-catenin protein levels and in HFF cells treated with PBS, HUMSCs-MVs, or DEX using Western blotting. We also determined the MMP1, MMP3, TIMP3, and TIMP4 levels using RT-PCR assay. The results showed that both NF-kB p65 and β-catenin protein levels were decreased in the groups of HUMSCs-MVs and DEX (Figure 9(a)–9(c)). They were even lower in the group of HUMSCs-MVs than those in the group of DEX (Figure 9(a)–9(c)). The MMP-1, MMP-3, and TIMP-3 (Figure 10(a)–10(c)) mRNA levels were significantly increased, and the TIMP-4 mRNA level was significantly decreased (Figure 10(d)) in the HUMSCs-MVs and DEX groups. The magnitude of changes in the MMP-1, MMP-3 (Figures 10(a) and10(b)), TIMP-3 (Figure 10(c)), and TIMP-4 (Figure 10(d)) mRNA levels were higher in the group of HUMSCs-MVs than those in the group of DEX. These results suggested that HUMSCs-MVs decreased NF-kB p65/β-catenin signaling and modulated MMPs and TIMPs levels in HFF cells.

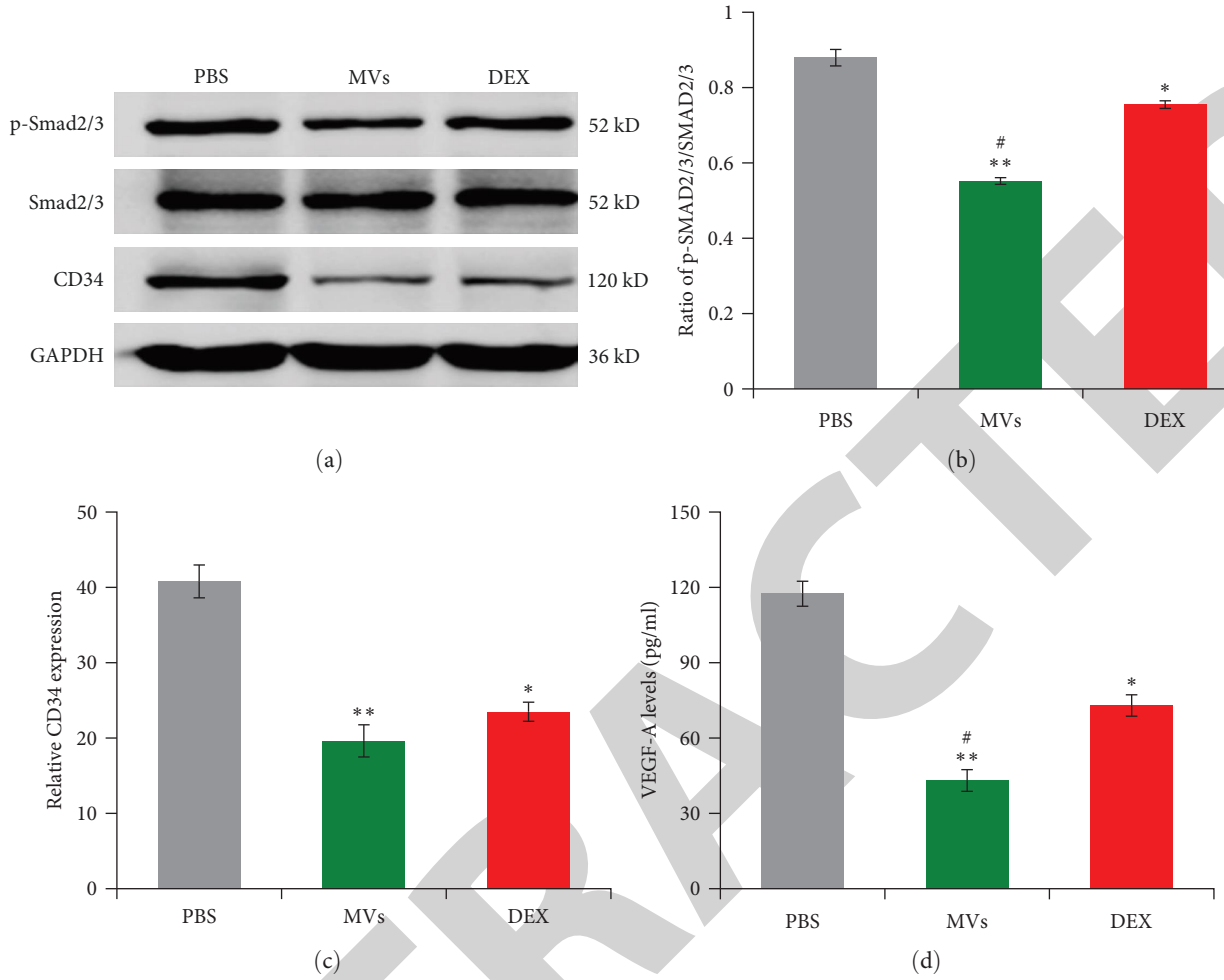

Figure 8: HUMSCs-MVs decreased phosphorylation of SMAD2/3 (P-SMAD2/3) and CD34 and VEGF-A expression in HFF cells. HFF cells were treated with PBS, HUMSCs-MVs, and DEX and subjected to determination of the SMAD2/3, p-SMAD2/3, CD34, and GAPDH protein levels using Western blotting and determination of the VEGF-A levels using ELISA. (a) SMAD2/3, p-SMAD2/3, CD34, and GAPDH were determined using Western blotting. GAPDH was used as a loading control. (b) Quantitation analysis of ratios of p-SMAD2/3/SMAD2/3 in the results of Western blotting. (c) Quantitation analysis of the CD34 protein levels in the results of Western blotting. (d) The VEGF-A levels in HFF cells treated with PBS, HUMSCs-MVs, and DEX. $^{*}P<0.05$ and $^{**}P<0.01$ compared with the PBS group. $\#P<0.05$ compared with the DEX group.

4. Discussion

In the current study, we prepared MVs from the medium of HUMSCs cultures. We found that HUMSCs-MVs reduced formation of hypertrophic scar tissues in a rabbit model based on appearance observation, and H&E staining, Masson staining, and immunohistochemical staining. The results support that HUMSCs-MVs have ameliorative effects on formation of hypertrophic scar during wound healing. This is consistent with the results of extracellular vesicles derived from human adipose-derived stem cell [21]. Furthermore, the efficacy of HUMSCs-MVs is better than that of DEX. Therefore, HUMSCs-MVs is a potential promising drug for formation of hypertrophic scar during wound healing.

Migration of abnormal types and numbers of cells and invasion of fast proliferation of fibroblasts in wound healing tissues are characteristics of hypertrophic scars [5–7, 46], as observed in the H&E staining results in the current study. In addition, our data reveal that HUMSCs-MVs inhibits invasion of HFF cells and decreases the levels of the α-SMA, N-WASP, cortacin proteins that are biomarkers for cell invasion. HUMSCs-MVs also inhibits cell proliferation of HFF cells. The effects of HUMSCs-MVs on invasion of HFF cells are comparable to or even better than those of DEX. Therefore, inhibiting proliferation and invasion of fibrotic cells is likely a mechanism of attenuative effects of HUMSCs-MVs on hypertrophic scar formation.

Chronic inflammation is a key factor contributing to formation of hypertrophic scars [6, 7]. Oxidative stress is intertwined with inflammation [55, 56] and associated with hypertrophic scar formation [42]. MMPs and TIMPs are key components of tissue remodeling in inflammation [52–54]. NF-kB is a master regulator of genes involved in inflammation [49, 50]. β-catenin is the downstream component of Wnt/β-catenin pathway that crosstalks with NF-kB signaling pathway during inflammation [51]. Increased β-catenin is associated with inflammation in many disease conditions, such as asthma and hepatocellular carcinoma, and becomes

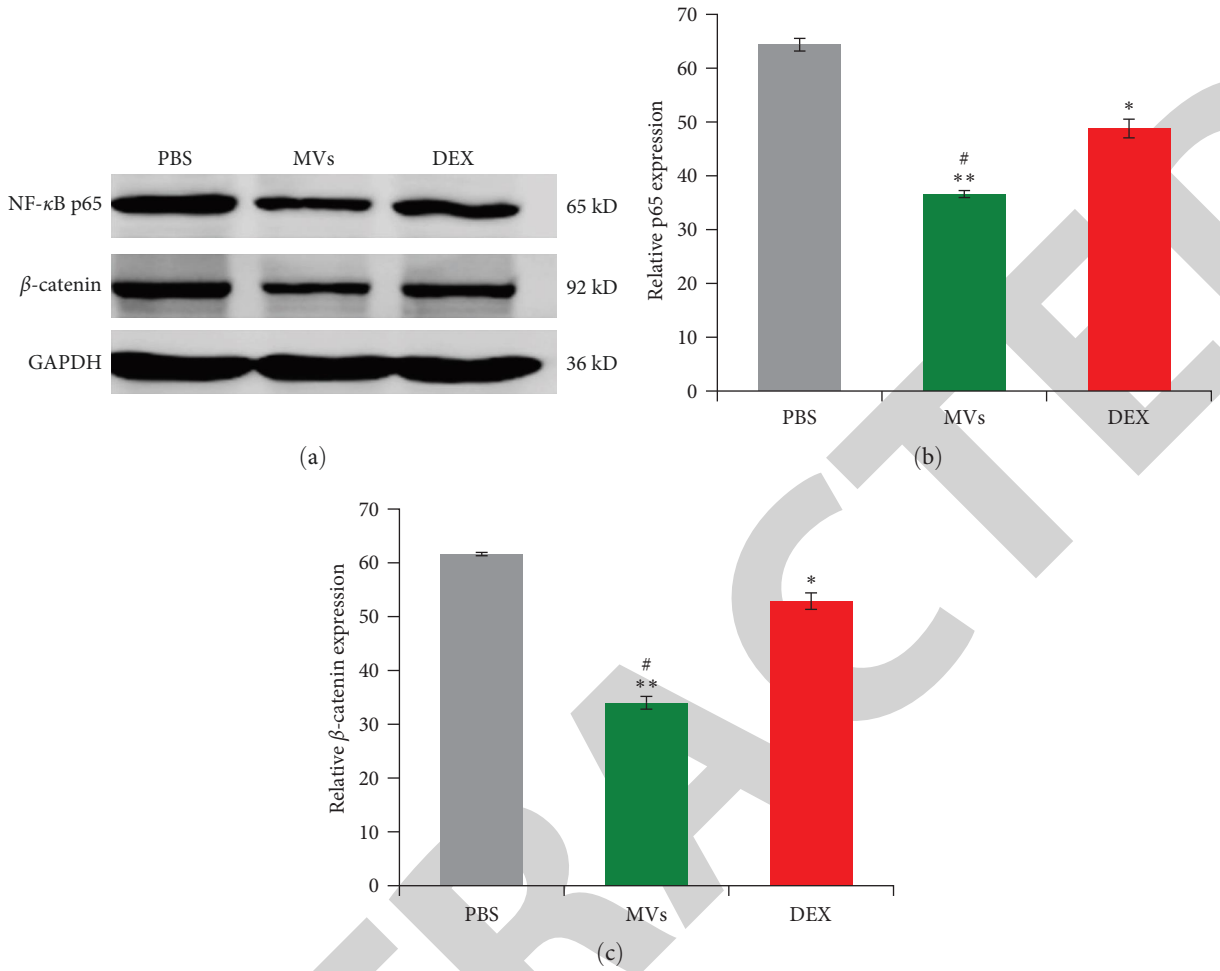

FIGURE 9: HUMSCs-MVs decreased NF-kB p65 and β-catenin expression in HFF cells. HFF cells were treated with PBS, HUMSCs-MVs, and DEX and subjected to determination of the NF-kB p65, β-catenin, and GAPDH protein levels using Western blotting. (a) NF-kB p65, β-catenin, and GAPDH protein levels were determined using Western blotting. GAPDH was used as loading control. (b) Quantitation analysis of NF-kB p65 in the results of Western blotting. (c) Quantitation analysis of the β-catenin protein levels in the results of Western blotting. $^{*}P<0.05$ and $^{**}P<0.01$ compared with the PBS group. $\#P<0.05$ compared with the DEX group.

the target to reduce inflammation [57, 58]. In the current study, we found that the MMP-1, MMP-3, and TIMP-3 mRNA levels are significantly increased, and the TIMP-4 mRNA level and the NF-kB p65/β-catenin protein levels are decreased in HFF cells after HUMSCs-MVs treatment. The magnitudes of changes are significantly higher than those of DEX. HUMSCs-MVs inhibited oxidative stress in hypertrophic scar tissues, as revealed by decreased MDA levels and Nrf2 expression levels, and increased SOD activity in hypertrophic scar tissues after HUMSCs-MVs treatment. The effects of HUMSCs-MVs on oxidative stress are comparable to or even better than those of DEX. Therefore, inhibiting inflammation and oxidative stress is likely a mechanism of attenuative effects of HUMSCs-MVs on hypertrophic scar formation.

Hypertrophic scar formation is characterized by disorder in ECM deposition and remodeling and excessive fibrosis [5–7]. Smad signaling pathway is the most canonical pathway involved in collagen production and hypertrophic scars formation [43]. In the current study, we found that HUMSCs-MVs promotes organization of collagen fibers in the rabbit ear model of collagen fibers. The p-SMAD2/3 levels and the ratios of p-SMAD2/3/SMAD2/3 were significantly decreased in both the wound healing tissues and HFF cells after HUMSCs-MVs and DEX treatment. The magnitudes of changes are significantly higher than those of DEX. It seems that suppressing p-SMAD2/3 is likely a mechanism of attenuative effects of HUMSCs-MVs on hypertrophic scar formation.

Abnormal angiogenesis is a key process that plays critical role in early stage of formation of hypertrophic scar [5–7]. CD34 is a biomarker and involved in initial angiogenesis [44, 45], and VEGF-A is a key regulator of angiogenesis [47, 48]. In the current study, we found that CD34 levels are significantly decreased in both wound healing scar tissues in the rabbit ear model and the HFF cell model after HUMSCs-MVs treatment. The VEGF-A level is also significantly decreased in the HFF cell model after HUMSCs-MVs treatment. The magnitudes of decreases are significantly or tend to be significantly lower than those of the DEX group. It is likely that HUMSCs-MVs attenuate hypertrophic scar formation through inhibiting angiogenesis.

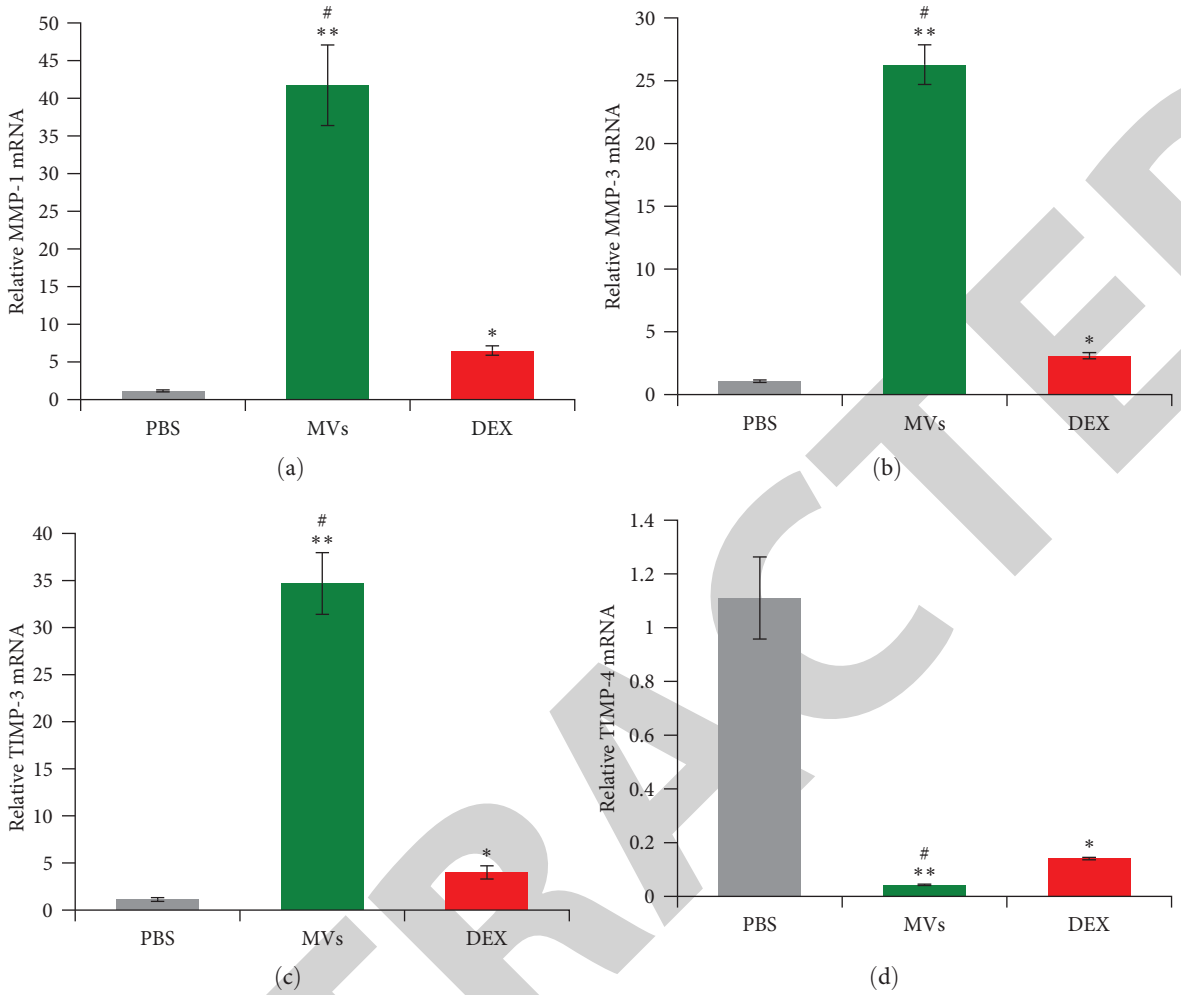

Figure 10: HUMSCs-MVs regulated expression of MMPs and TIMPs in HFF cells. HFF cells were treated with PBS, HUMSCs-MVs, and DEX and then were collected. Total RNAs were extracted and subjected to RT-PCR analysis. The relative expression levels of MMP-1 (a), MMP-3 (b), TIMP-3 (c), and TIMP-4 (d) were calculated and compared among PBS, HUMSCs-MVs, and DEX treatments. $^{*}P<0.05$ and $^{**}P<0.01$ compared with the PBS group. $\#P<0.05$ compared with the DEX group.

5. Conclusion

In the current study, we used a rabbit ear model and a foreskin fibroblast model to investigate the effects and the underlying mechanism of HUMSCs-MVs on formation of hypertrophic scars. Our data indicated that HUMSCs-MVs effectively reduce the formation of hypertrophic scar tissues probably through inhibiting viability and invasion of fibroblasts, resolving inflammation and reducing oxidative stress, suppressing Smad2/3 signaling, and reducing angiogenesis (Figure 11). Since HUMSCs has several advantages in differentiative potential, immune-rejection, availability [22–25], and extracellular vesicles are safer for the lack of proliferation and migration of live cells. Therefore, HUMSCs-MVs is a potential promising drug to attenuate formation of hypertrophic scar during wound healing.

Data Availability

The datasets used and/or analyzed during current study are available from corresponding author upon reasonable request.

Ethical Approval

All above procedures for care and use of animals were approved by the Ethical Committee of Zhongnan Hospital of Wuhan University, Wuhan, China (no. ZN2021017). The animal experiments were conducted according to the Guidelines of Declaration of Helsinki and all applicable institutional and governmental regulations concerning the ethical use of animals were followed.

Disclosure

No funding source had any role in study design, data collection, analysis, interpretation, writing of the report, or decision to submit the paper for publication.

Conflicts of Interest

The authors declare that they have no conflicts of interest.

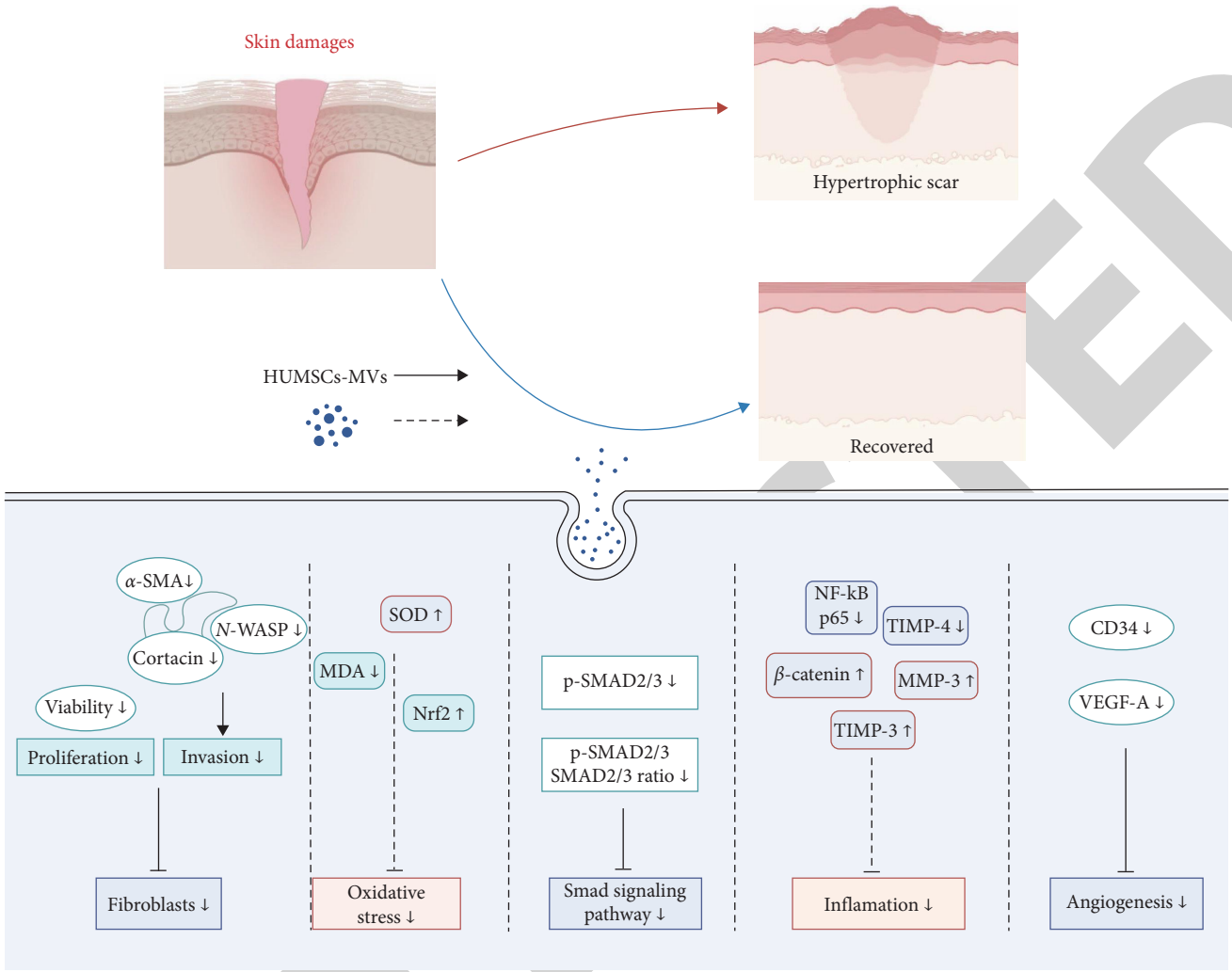

Figure 11: Mechanism underlying the effect of HUMSCs-MVs on attenuating formation of hypertrophic scars.

Authors' Contributions

Qun Qian and Weicheng Liu conceived and designed this research; Ni Zhu, Wenzhe Li, and Songlin Wan performed all experiments; Ni Zhu and Dongcheng Wu analyzed data; Ni Zhu, Wenzhe Li, and Songlin Wan interpreted results of all experiments; Ni Zhu, Wenzhe Li, and Songlin Wan prepared figures; Ni Zhu, Wenzhe Li, Songlin Wan, and Yunhua Wu drafted the manuscript; Qun Qian and Weicheng Liu edited and revised the manuscript. All authors approved final version of manuscript.

Qun Qian, Ni Zhu, Wenzhe Li, and Songlin Wan contributed equally to this study.

Acknowledgments

This study was funded by the National Natural Science Foundation of China (no. 81500505) and the Medical Science and Technology Innovation Platform of Health Commission of Hubei Province/Zhongnan Hospital of Wuhan University (no. PTXM2021025).

References

[1] B. Lukomska, L. Stanaszek, E. Zuba-Surma, P. Legosz, S. Sarzynska, and K. Drela, "Challenges and controversies in human mesenchymal stem cell therapy," *Stem Cells International*, vol. 2019, Article ID 9628536, 10 pages, 2019.

[2] J. Vasanthan, N. Gurusamy, S. Rajasingh et al., "Role of human mesenchymal stem cells in regenerative therapy," *Cells*, vol. 10, no. 1, Article ID 54, 2020.

[3] R. Stavely and K. Nurgali, "The emerging antioxidant paradigm of mesenchymal stem cell therapy," *Stem Cells Translational Medicine*, vol. 9, no. 9, pp. 985–1006, 2020.

[4] R. A. Poltavtseva, A. V. Poltavtsev, G. V. Lutsenko, and E. V. Svirshchevskaya, "Myths, reality and future of mesenchymal stem cell therapy," *Cell and Tissue Research*, vol. 375, pp. 563–574, 2019.

[5] V. Sarrazy, F. Billet, L. Micallef, B. Coulomb, and A. Desmoulière, "Mechanisms of pathological scarring: role of myofibroblasts and current developments," *Wound Repair and Regeneration*, vol. 19, no. s1, pp. s10–s15, 2011.

[6] C. Huang and R. Ogawa, "Systemic factors that shape cutaneous pathological scarring," *The FASEB Journal*, vol. 34, no. 10, pp. 13171–13184, 2020.

[7] S.-M. Karppinen, R. Heljasvaara, D. Gullberg, K. Tasanen, and T. Pihlajaniemi, "Toward understanding scarless skin wound healing and pathological scarring [version 1; peer review: 2 approved]," *F1000Research*, vol. 8, no. F1000 Faculty Rev, Article ID 787, 2019.

[8] S. P. Nischwitz, K. Rauch, H. Luze et al., "Evidence-based therapy in hypertrophic scars: an update of a systematic review," *Wound Repair and Regeneration*, vol. 28, no. 5, pp. 656–665, 2020.

[9] J. Zuccaro, N. Ziolkowski, and J. Fish, "A systematic review of the effectiveness of laser therapy for hypertrophic burn scars," *Clinics in Plastic Surgery*, vol. 44, no. 4, pp. 767–779, 2017.

[10] A. Nast, G. Gauglitz, K. Lorenz et al., "S2k guidelines for the therapy of pathological scars (hypertrophic scars and keloids) —update 2020," *JDDG: Journal der Deutschen Dermatologischen Gesellschaft*, vol. 19, no. 2, pp. 312–327, 2021.

[11] S. Gupta and V. K. Sharma, "Standard guidelines of care: keloids and hypertrophic scars," *Indian Journal of Dermatology, Venereology, and Leprology*, vol. 77, no. 1, pp. 94–100, 2011.

[12] F. Xie, L. Teng, J. Xu et al., "Adipose-derived mesenchymal stem cells inhibit cell proliferation and migration and suppress extracellular matrix synthesis in hypertrophic-scar and keloid fibroblasts," *Experimental and Therapeutic Medicine*, vol. 21, no. 2, Article ID 139, 2021.

[13] J. Deng, Y. Shi, Z. Gao et al., "Inhibition of pathological phenotype of hypertrophic scar fibroblasts via coculture with adipose-derived stem cells," *Tissue Engineering Part A*, vol. 24, no. 5-6, pp. 382–393, 2018.

[14] S. Liu, L. Jiang, H. Li et al., "Mesenchymal stem cells prevent hypertrophic scar formation via inflammatory regulation when undergoing apoptosis," *Journal of Investigative Dermatology*, vol. 134, no. 10, pp. 2648–2657, 2014.

[15] C. Bojanic, K. To, A. Hatoum et al., "Mesenchymal stem cell therapy in hypertrophic and keloid scars," *Cell and Tissue Research*, vol. 383, pp. 915–930, 2021.

[16] K. T. Putri and T. O. H. Prasetyono, "A critical review on the potential role of adipose-derived stem cells for future treatment of hypertrophic scars," *Journal of Cosmetic Dermatology*, vol. 21, no. 5, pp. 1913–1919, 2022.

[17] X. He, J. Zhang, L. Luo, J. Shi, and D. Hu, "New progress of adipose-derived stem cells in the therapy of hypertrophic scars," *Current Stem Cell Research & Therapy*, vol. 15, no. 1, pp. 77–85, 2020.

[18] C.-H. Hu, Y.-W. Tseng, C.-Y. Chiou et al., "Bone marrow concentrate-induced mesenchymal stem cell conditioned medium facilitates wound healing and prevents hypertrophic scar formation in a rabbit ear model," *Stem Cell Research & Therapy*, vol. 10, Article ID 275, 2019.

[19] C.-Y. Chai, J. Song, Z. Tan, I.-C. Tai, C. Zhang, and S. Sun, "Adipose tissue-derived stem cells inhibit hypertrophic scar (HS) fibrosis via p38/MAPK pathway," *Journal of Cellular Biochemistry*, vol. 120, no. 3, pp. 4057–4064, 2019.

[20] X. Meng, X. Gao, X. Chen, and J. Yu, "Umbilical cord-derived mesenchymal stem cells exert anti-fibrotic action on hypertrophic scar-derived fibroblasts in co-culture by inhibiting the activation of the TGF β1/Smad3 pathway," *Experimental and Therapeutic Medicine*, vol. 21, no. 3, Article ID 210, 2021.

[21] Y.-Z. Zhu, X. Hu, J. Zhang, Z.-H. Wang, S. Wu, and Y.-Y. Yi, "Extracellular vesicles derived from human adipose-derived stem cell prevent the formation of hypertrophic scar in a rabbit model," *Annals of Plastic Surgery*, vol. 84, no. 5, pp. 602–607, 2020.

[22] M. Mebarki, C. Abadie, J. Larghero, and A. Cras, "Human umbilical cord-derived mesenchymal stem/stromal cells: a promising candidate for the development of advanced therapy medicinal products," *Stem Cell Research & Therapy*, vol. 12, Article ID 152, 2021.

[23] L. Marino, M. A. Castaldi, R. Rosamilio et al., "Mesenchymal stem cells from the wharton's jelly of the human umbilical cord: biological properties and therapeutic potential," *International Journal of Stem Cells*, vol. 12, pp. 218–226, 2019.

[24] S. Sriramulu, A. Banerjee, R. Di Liddo et al., "Concise review on clinical applications of conditioned medium derived from human umbilical cord-mesenchymal stem cells (UC-MSCs)," *International Journal of Hematology-Oncology and Stem Cell Research*, vol. 12, no. 3, pp. 230–234, 2018.

[25] T. Li, M. Xia, Y. Gao, Y. Chen, and Y. Xu, "Human umbilical cord mesenchymal stem cells: an overview of their potential in cell-based therapy," *Expert Opinion on Biological Therapy*, vol. 15, no. 9, pp. 1293–1306, 2015.

[26] O. Kloeters, A. Tandara, and T. A. Mustoe, "Hypertrophic scar model in the rabbit ear: a reproducible model for studying scar tissue behavior with new observations on silicone gel sheeting for scar reduction," *Wound Repair and Regeneration*, vol. 15, no. s1, pp. S40–S45, 2007.

[27] S. Tang, B. Cai, H. Xu et al., "[The influence of Matrine on apoptosis of fibroblasts and the expression of apoptotic modulation related protein in hypertrophic scar of rabbit ear]," *Zhonghua Shao Shang Za Zhi*, vol. 18, no. 5, pp. 299–301, 2002.

[28] S. M. Mousavizadeh, P. M. Torbati, and A. Daryani, "The effects of kiwifruit dressing on hypertrophic scars in a rabbit ear model," *Journal of Wound Care*, vol. 30, no. Sup9a, pp. XVi–XVvii, 2021.

[29] P. Bainbridge, "Wound healing and the role of fibroblasts," *Journal of Wound Care*, vol. 22, no. 8, pp. 407–412, 2013.

[30] A. Stunova and L. Vistejnova, "Dermal fibroblasts—a heterogeneous population with regulatory function in wound healing," *Cytokine & Growth Factor Reviews*, vol. 39, pp. 137–150, 2018.

[31] T. Oliveira, I. Costa, V. Marinho et al., "Human foreskin fibroblasts: from waste bag to important biomedical applications," *Journal of Clinical Urology*, vol. 11, no. 6, pp. 385–394, 2018.

[32] C. A. Nadalutti and S. H. Wilson, "Using human primary foreskin fibroblasts to study cellular damage and mitochondrial dysfunction," *Current Protocols in Toxicology*, vol. 86, no. 1, Article ID e99, 2020.

[33] L. L. Ramenzoni, F. E. Weber, T. Attin, and P. R. Schmidlin, "Cerium chloride application promotes wound healing and cell proliferation in human foreskin fibroblasts," *Materials*, vol. 10, no. 6, Article ID 573, 2017.

[34] M. A. Carlson, A. K. Prall, J. J. Gums, A. Lesiak, and V. K. Shostrom, "Biologic variability of human foreskin fibroblasts in 2D and 3D culture: implications for a wound healing model," *BMC Research Notes*, vol. 2, Article ID 229, 2009.

[35] Z. Yang, X. Du, C. Wang et al., "Therapeutic effects of human umbilical cord mesenchymal stem cell-derived microvesicles on premature ovarian insufficiency in mice," *Stem Cell Research & Therapy*, vol. 10, Article ID 250, 2019.

[36] C. Théry, S. Amigorena, G. Raposo, and A. Clayton, "Isolation and characterization of exosomes from cell culture supernatants and biological fluids," *Current Protocols in Cell Biology*, vol. 30, pp. 3.22.1–3.22.29, 2006.

[37] D. E. Morris, L. Wu, L. L. Zhao et al., "Acute and chronic animal models for excessive dermal scarring: quantitative studies," *Plastic and Reconstructive Surgery*, vol. 100, no. 3, pp. 674–681, 1997.

[38] N. Zhou, D. Li, Y. Luo, J. Li, and Y. Wang, "Effects of botulinum toxin type a on microvessels in hypertrophic scar models on rabbit ears," *BioMed Research International*, vol. 2020, Article ID 2170750, 7 pages, 2020.

[39] F. Syed, R. A. Bagabir, R. Paus, and A. Bayat, "*Ex vivo* evaluation of antifibrotic compounds in skin scarring: EGCG and silencing of PAI-1 independently inhibit growth and induce keloid shrinkage," *Laboratory Investigation*, vol. 93, no. 8, pp. 946–960, 2013.

[40] A. N. Rout, K. Sahu, and C. S. Sirka, "Pyoderma gangrenosum over hypertrophic scar: report of a rare presentation," *Indian Dermatology Online Journal*, vol. 11, no. 2, pp. 222–225, 2020.

[41] W. M. van der Veer, J. A. Ferreira, E. H. de Jong, G. Molema, and F. B. Niessen, "Perioperative conditions affect long-term hypertrophic scar formation," *Annals of Plastic Surgery*, vol. 65, no. 3, pp. 321–325, 2010.

[42] Y. Feng, J.-J. Wu, Z.-L. Sun et al., "Targeted apoptosis of myofibroblasts by elesclomol inhibits hypertrophic scar formation," *EBioMedicine*, vol. 54, Article ID 102715, 2020.

[43] T. Zhang, X.-F. Wang, Z.-C. Wang et al., "Current potential therapeutic strategies targeting the TGF-β/Smad signaling pathway to attenuate keloid and hypertrophic scar formation," *Biomedicine & Pharmacotherapy*, vol. 129, Article ID 110287, 2020.

[44] L. Díaz-Flores, R. Gutiérrez, M. P. García et al., "Comparison of the behavior of perivascular cells (pericytes and CD34+ stromal cell/telocytes) in sprouting and intussusceptive angiogenesis," *International Journal of Molecular Sciences*, vol. 23, no. 16, Article ID 9010, 2022.

[45] A. Kawamoto, H. Iwasaki, K. Kusano et al., "CD34-positive cells exhibit increased potency and safety for therapeutic neovascularization after myocardial infarction compared with total mononuclear cells," *Circulation*, vol. 114, no. 20, pp. 2163–2169, 2006.

[46] R. Ţuţuianu, A. M. Roşca, G. Florea et al., "Heterogeneity of human fibroblasts isolated from hypertrophic scar," *Romanian Journal of Morphology and Embryology*, vol. 60, no. 3, pp. 793–802, 2019.

[47] J. A. Nagy, A. M. Dvorak, and H. F. Dvorak, "VEGF-A and the induction of pathological angiogenesis," *Annual Review of Pathology: Mechanisms of Disease*, vol. 2, pp. 251–275, 2007.

[48] P. Kapoor and R. S. Deshmukh, "VEGF: a critical driver for angiogenesis and subsequent tumor growth: an IHC study," *Journal of Oral & Maxillofacial Pathology*, vol. 16, no. 3, pp. 330–337, 2012.

[49] T. Lawrence, "The nuclear factor NF-κB pathway in inflammation," *Cold Spring Harbor Perspectives in Biology*, vol. 1, Article ID a001651, 2009.

[50] P. J. Barnes and M. Karin, "Nuclear factor-κB—a pivotal transcription factor in chronic inflammatory diseases," *New England Journal of Medicine*, vol. 336, pp. 1066–1071, 1997.

[51] B. Ma and M. O. Hottiger, "Crosstalk between Wnt/β-catenin and NF-κB signaling pathway during inflammation," *Frontiers in Immunology*, vol. 7, Article ID 378, 2016.

[52] G. S. Butler and C. M. Overall, "Matrix metalloproteinase processing of signaling molecules to regulate inflammation," *Periodontology 2000*, vol. 63, no. 1, pp. 123–148, 2013.

[53] L. Nissinen and V.-M. Kähäri, "Matrix metalloproteinases in inflammation," *Biochimica et Biophysica Acta (BBA) - General Subjects*, vol. 1840, no. 8, pp. 2571–2580, 2014.

[54] A. M. Manicone and J. K. McGuire, "Matrix metalloproteinases as modulators of inflammation," *Seminars in Cell & Developmental Biology*, vol. 19, no. 1, pp. 34–41, 2008.

[55] G. Verdile, K. N. Keane, V. F. Cruzat et al., "Inflammation and oxidative stress: the molecular connectivity between insulin resistance, obesity, and Alzheimer's disease," *Mediators of Inflammation*, vol. 2015, p. 17, Article ID 105828, 2015.

[56] S. Nowsheen, K. Aziz, T. B. Kryston, N. F. Ferguson, and A. Georgakilas, "The interplay between inflammation and oxidative stress in carcinogenesis," *Current Molecular Medicine*, vol. 12, no. 6, pp. 672–680, 2012.

[57] R. Huo, X. Tian, Q. Chang et al., "Targeted inhibition of β-catenin alleviates airway inflammation and remodeling in asthma *via* modulating the profibrotic and anti-inflammatory actions of transforming growth factor-β_1," *Therapeutic Advances in Respiratory Disease*, vol. 15, pp. 1–14, 2021.

[58] H. M. Hassan, S. M. H. El-Kannishy, A. Alattar, R. Alshaman, A. M. Hamdan, and M. M. H. Al-Gayyar, "Therapeutic effects of blocking β-catenin against hepatocellular carcinoma-induced activation of inflammation, fibrosis and tumor invasion," *Biomedicine & Pharmacotherapy*, vol. 135, Article ID 111216, 2021.